Auxiliary Part of Ligand Mediated Unique Coordination Chemistry of Copper (II)

Ishani Majumder,[a] Prateeti Chakraborty,*[b] Jaydeep Adhikary,[a] Hulya Kara,[c, d] Ennio Zangrando,*[e] Antonio Bauza,[f] Antonio Frontera,*[f] and Debasis Das*[a]

Six N,N,O-donor Schiff-base ligands, HL1-HL6, [HL1/HL2/HL3 = {2-(2-piperazin-1-yl)ethylimino)methyl)-4-(Cl/H/Me)-phenol}; HL4/HL5/HL6 = {2-(2-morpholine/piperidine/ pyrrolidine −1-yl) ethylimino)methyl)-4-chlorophenol}, have been designed by combining 5-R-2-hydroxy-benzaldehyde, (R=Cl/H/Me) and N-(2-aminoethyl)-Y, (Y = piperazin/morpholine/ piperidine/pyrrolidine) with the view to explore the role of R and X (part of Y excluding coordinating N) on the coordination chemistry of Cu (II) in presence of bromide as counter anion. HL1-HL6 formed in situ on reaction with $Cu(II)Br_2$ produce complexes **1–6**, respectively. Complex **1,** $[Cu(II)_2Cu(I)_2(L1)(MeOH)_2Br_{7.30}]$, is a mixed valence Cu(I)-Cu(II) species having phenyl ring brominated at ortho position with 0.65 occupancy. Complexes **2–4** are mononuclear species with general formula $[Cu\{L2/L3/L4)\}Br_2]$. Complexes $[Cu_3(L5)Br_4]$ (**5**) and $[Cu_3(L6)Br_4]$ (**6**) are trinuclear species having similar structure but exhibit different magnetic property, **5** is ferro- ($J = +16.64\ cm^{-1}$) and **6** is antiferromegnetic ($J = -11.76\ cm^{-1}$). The influence of R and X on bromonation, magnetic property and nuclearity issues have been rationalized by DFT calculations.

Introduction

Coordination chemistry stands on two main components: metal ion and ligand. Chemistry of a particular metal ion may largely be influenced by the ligand characteristics such as nature of the ligating site, number of the ligating atoms, chelate ring size, steric and electronic factors of the chelate ring, cavity size (for cyclic ligands) etc.[1–4] Schiff-base ligands take a vital role in developing coordination chemistry and in recent time tridentate acyclic Schiff-base ligands having N,N,O-donor sites attract special attention to the coordination chemists due to their greater flexibility. In our recent efforts with two homologous N,N,O-donor Schiff-base ligands we observed strikingly different reactivity upon complexation with Zn(II) in presence of different coordinating and non-coordinating anions. We noticed that the variation of the ligand backbone plays a key role in the different behaviours observed, as evidenced by DFT calculations.[5,6] Those notable findings inspired us to explore the influence of the atom or group of atoms which is present in the ligand periphery but apparently has no effect on ligating backbone or on the chelating property of the ligand and is not directly linked with the coordination environment of the metal ion. We may refer that particular portion (atom or group of atoms) as "auxiliary part" of the ligand. Consequently, we have designed six ligands HL1-HL6, where we have added auxiliary parts, R and X (Scheme 1). We have adopted two strategies to evaluate the influence of R and X separately on the coordination chemistry of copper(II) using bromide as co-ligand. Our first step was to use ligands HL1-HL3 to establish a metal complex with $Cu(II)Br_2$. By using this synthetic strategy, R (R=Cl, Complex **1**; R = H, complex **2** and R=CH_3, complex **3**) is being varied while X remained constant. Remarkably, for complex **1** the reaction proceeds with bromination on the aromatic ring. A similar observation was reported by Chen *at el.*, showing evidences of hydroxylation on the ligand backbone.[7] A literature survey reveals that $Cu(II)Br_2$ is extensively used for the α-bromination of carbonyl compounds and bromination of alkenes and alkynes,[8–11] however, very few studies highlight the possibility to use it as a brominating agent in aromatic systems.[10–11] In the first step of our study we obtained the product of the aromatic bromination and analyzed the influence of the auxiliary part of the ligand by means of DFT calculations. In the second step,

[a] *I. Majumder, J. Adhikary, Prof. D. Das*
Department of Chemistry,
University of Calcutta,
92, A. P. C. Road, Kolkata – 700009, India
E-mail: dasdebasis2001@yahoo.com
[b] *Dr. P. Chakraborty*
Department of Chemistry,
Amity University,
Newtown, Kolkata, 700156, India
E-mail: prateeti_17@yahoo.co.in
[c] *Prof. H. Kara*
Department of Physics,
Faculty of Science and Art,
Balikesir University, 10145 Balikesir, Turkey
[d] *Prof. H. Kara*
Department of Physics,
Faculty of Science, Mugla Sıtkı Koçman University,
Mugla, Turkey
[e] *Prof. E. Zangrando*
Department of Chemical and Pharmaceutical Sciences,
University of Trieste,
Via L. Giorgieri 1, 34127 Trieste, Italy
E-mail: ezangrando@units.it
[f] *A. Bauza, Prof. A. Frontera*
Departament de Química,
Universitat de les Illes Balears,
Crta. de Valldemossa km 7.5, 07122, Palma (Baleares), Spain
E-mail: toni.frontera@uib.es

Supporting information for this article is available on the WWW under http://dx.doi.org/10.1002/slct.201500030

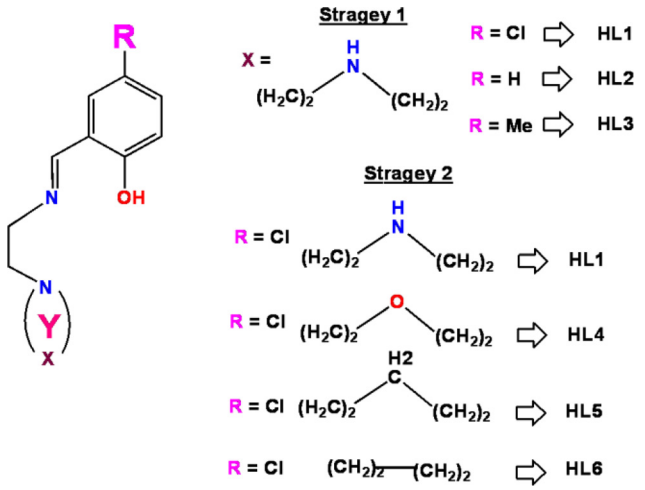

Scheme 1. Ligands used for present investigation.

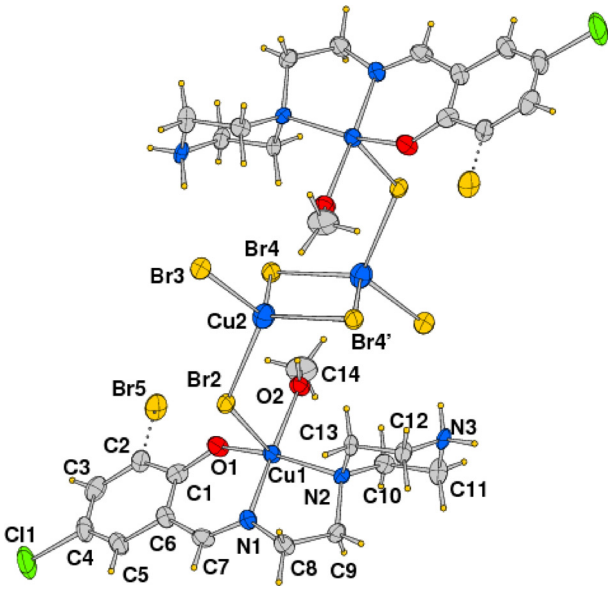

Figure 1. ORTEP drawing (40% probability ellipsoids) of complex **1** with label scheme of the crystallographic independent unit.

bearing in mind R and X as denoted in Scheme 1, we have kept R fixed as Cl and varied X. These strategy leads to the ligands HL1 and HL4-HL6. Which on reaction with Cu(II)Br_2 produce a tetranuclear mixed valence copper(I)-copper(II) complex (**1**), a mononuclear square planar species (**4**) and two trinuclear complexes, **5** and **6**, respectively. Complexes **5** and **6** have very similar structural features but exhibit different magnetic behavior. DFT calculations have been performed to rationalize the observed experimental facts and all those experimental observations and theoretical rationalizations have been vividly portrayed in this manuscript.

Results and Discussion

Synthesis, Rationalization, and Characterization of the Metal-Complexes.

Complexes **1–6** are synthesized by adopting template synthesis technique by treating methanolic solution of copper (II) bromide with Schiff-base ligands formed in situ via condensation of the aldehydes and amines. In all cases single crystals suitable for X-ray analysis are obtained.

Crystal Structure Descriptions

Complex **1** crystallizes as a mixed valence, centrosymmetric dimer, resulting in a tetranuclear cluster as depicted in Figure 1. Each dimer contains one crystallographic unique divalent copper ion, Cu(1), and a monovalent one, Cu(2) occurring in a five-, and four- coordination sphere, respectively. The divalent copper ion is in a distorted square pyramidal coordination environment, being chelated by the Schiff base and completing the coordination sphere with a methanol molecule and a bromine at the apex of the pyramid. The basal Cu (1)-O bond distances are of 1.895(5) and 1.975(5) Å, the Cu (1)-N ones of 1.907(6) and 2.076(5) Å, where the latter slightly longer value pertains to the piperidine amino nitrogen. In addition a long Cu(1)-Br(2) bond of 2.8540(14) Å is measured for the apical site. The monovalent copper ion is tetrahedrally coordinated with Cu(2)-Br bond lengths ranging from 2.4263(14) to 2.5503(15) Å, forming a $[Cu_2Br_6]^{4-}$ anion, located on a crystallographic center of symmetry. It is worth of note that the phenolato ring was brominated in ortho position and the structural analysis indicate the presence of a disordered situation where bromine Br(5) has occupancy of ca. 0.65. The protonated amino group $N(3)H_2$ shows an intramolecular interaction with Br(3) and with Br(2) of a symmetry related unit (N…Br = 3.388(6)and 3.346(6)Å, respectively).

Table 1. Coordination bond distances (Å) and angles (°) for complex **1.**

Cu(1)-O(1)	1.895(5)	Cu(2)-Br(2)	2.5194(15)
Cu(1)-O(2)	1.975(5)	Cu(2)-Br(3)	2.4263(14)
Cu(1)-N(1)	1.907(6)	Cu(2)-Br(4)	2.5148(18)
Cu(1)-N(2)	2.076(5)	Cu(2)-Br(4′)	2.5503(15)
Cu(1)-Br(2)	2.8540(14)		
O(1)-Cu(1)-N(1)	93.5(2)	N(2)-Cu(1)-Br(2)	100.51(15)
O(1)-Cu(1)-O(2)	89.3(2)	Br(4)-Cu(2)-Br(2)	114.64(4)
N(1)-Cu(1)-O(2)	177.2(2)	Br(3)-Cu(2)-Br(4)	117.22(6)
O(1)-Cu(1)-N(2)	160.1(2)	Br(3)-Cu(2)-Br(4′)	107.97(5)
N(1)-Cu(1)-N(2)	85.4(2)	Br(3)-Cu(2)-Br(2)	107.76(5)
O(2)-Cu(1)-N(2)	91.9(2)	Br(4)-Cu(2)-Br(4′)	105.42(4)
O(1)-Cu(1)-Br(2)	99.39(15)	Br(2)-Cu(2)-Br(4′)	102.61(5)
N(1)-Cu(1)-Br(2)	90.38(16)	Cu(1)-Br(2)-Cu(2)	114.72(4)
O(2)-Cu(1)-Br(2)	89.38(14)	Cu(2)-Br(4)-Cu(2′)	74.58(4)

Primed atoms at -x,-y+1,-z+1

Complexes **2–3** are mononuclear species where copper (II) ion exhibits a square pyramidal coordination sphere, being chelated by the tridentate Schiff base ligand through the phenolato oxygen, the imino and the amino nitrogen completing the coordination sphere with bromides. The ORTEP drawing of

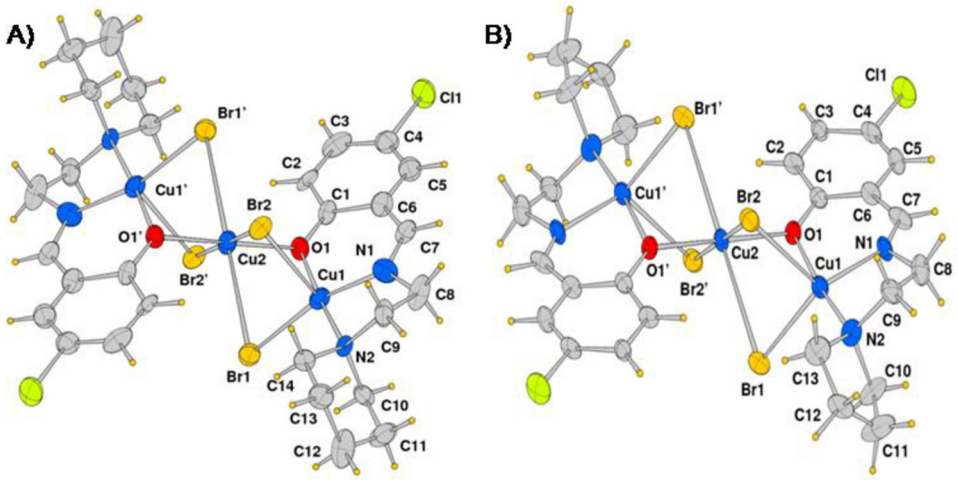

Figure 4. ORTEP drawing (40 % probability ellipsoids) of one of the two centrosymmetric complexes in compound **5** (A) (primed atoms at -x,-y + 2,–z + 1) and of complex **6** (B).

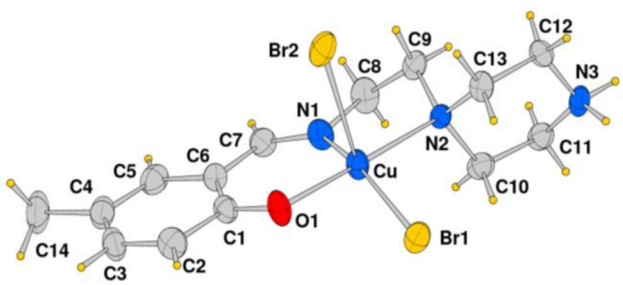

Figure 2. ORTEP drawing (40 % probability ellipsoids) of complex **3.** Same scheme is applied to complex **2** replacing methyl C14 with a H atom.

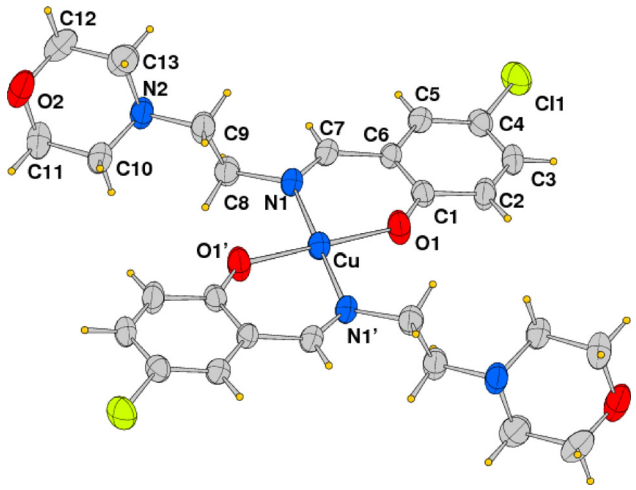

Figure 3. ORTEP drawing (40 % probability ellipsoids) of complex **4** with label scheme of the crystallographic independent part.

2 and **3** are shown in Figure. S19 and Figure 2 respectively, and pertinent bond distances and angles of the complexes reported as supplementary (Table S3). The square pyramidal geometry is confirmed by the τ value[12] which is 0.335 and 0.316, respectively. In both the complexes the Cu–O and Cu-N(imino) bond lengths are close comparable being 1.925(6), 1.953(5) Å and 1.937(8), 1.974(6) Å, respectively. On the other hand the Cu-N(piperazine) bond distance slightly differs in **2** and **3**, being 2.103(7) and 2.143(5)Å, respectively. As expected, the apical Cu–Br bond length is longer by ca 0.4 Å compared to the value measured for the halide in the basal plane (2.85 vs 2.44 Å, mean values in the two complexes). The piperazine has the expected chair conformation with the nitrogen atom N(3) protonated that, beside to guarantee the charge neutrality, is involved in H-bonds with the phenol oxygen and a bromide of a symmetry related complex.

Complex **4** is a centrosymmetric copper(II) bischelated species and the molecular structure is shown in Figure 3. In the discrete neutral complex the copper ion, located on a crystallographic inversion center, is coordinated by the phenolato oxygen and the imino nitrogen donor of two symmetry related ligands, while the morpholine rings remain uncoordinated. The Cu–O and the Cu–N bond lengths are of 1.884(3) and 2.036(3) Å, respectively with a chelating angle of 91.73(12)°. The coordination distances are slightly shorter and longer, respectively with respect to the values measured in complexes **2–3**, where the ligand acts as a tridentate .The same complex reported a few years ago,[13] and other species based on differently substituted phenols,[14] confirm the scarce propensity of morpholine to be not coordinated in close similar complexes.

Complexes **5** and **6** are close comparable centrosymmetric trinuclear species. Figure 4 depicts an ORTEP drawing of the neutral complexes and Table 2 shows pertinent coordination bond distances and angles. The crystallographic independent unit is formed by half complex and the unit cell of compound **5** contains two of these half dimers (complexes A and B). The complexes can be better described as built by two square pyramidal species embracing an additional copper ion through the bromine atoms and the phenoxo oxygen atoms in a centrosymmetric fashion. The side located copper (II) ions exhibit a square pyramidal coordination sphere, being chelated by the tridentate Schiff base through the phenolato oxygen, the imino and the amino nitrogen completing the coordination sphere with two bromides. The coordination bond distances of Cu (1) are comparable with those of the mononuclear complexes.

Table 2. Coordination bond distances (Å) and angles (°) for complexes **5** and **6.**

	5, complex A	**5**, complex B	**6**
Cu(1)-O(1)	1.976(16)	1.98(2)	1.969(13)
Cu(1)-N(1)	1.87(2)	1.899(19)	1.933(16)
Cu(1)-N(2)	2.09(2)	2.07(4)	2.020(17)
Cu(1)-Br(1)	2.453(6)	2.408(5)	2.436(4)
Cu(1)-Br(2)	2.748(6)	2.804(6)	2.769(4)
Cu(2)-O(1)	1.970(16)	1.99(2)	1.972(13)
Cu(2)-Br(1)	2.935(7)	2.934(7)	2.924(3)
Cu(2)-Br(2)	2.491(4)	2.489(3)	2.496(3)
Cu(1)-Cu(2)	2.973(4)	2.999(3)	2.992(3)
O(1)-Cu(1)-N(1)	92.7(8)	93.3(7)	90.2(6)
O(1)-Cu(1)-N(2)	174.9(10)	175.7(14)	172.3(7)
N(1)-Cu(1)-N(2)	83.3(9)	83.2(11)	84.8(7)
O(1)-Cu(1)-Br(1)	88.0(6)	87.4(6)	89.6(4)
N(1)-Cu(1)-Br(1)	159.7(10)	160.2(9)	152.0(6)
N(2)-Cu(1)-Br(1)	96.8(7)	95.0(10)	97.5(5)
O(1)-Cu(1)-Br(2)	77.2(8)	78.5(10)	76.8(4)
N(1)-Cu(1)-Br(2)	103.8(10)	105.7(9)	114.2(6)
N(2)-Cu(1)-Br(2)	100.7(8)	104.9(14)	99.9(5)
Br(1)-Cu(1)-Br(2)	96.16(17)	93.88(16)	92.95(11)
O(1)-Cu(2)-Br(2)	83.9(7)	86.5(8)	83.8(4)
O(1)-Cu(2)-Br(2′)	96.1(7)	93.5(8)	96.2(4)
Cu(2)-Br(2)-Cu(1)	68.94(14)	68.73(13)	69.03(8)

However the formation of these trinuclear species leads to a slight variation of the coordination geometry at Cu (1) and the most relevant is a narrowing of the Br(1)-Cu(1)-Br(2) bond angle from 106.4 to 94.3° (mean value of complexes **2–3** and **5–6**). On the other hand the central copper ion (Cu(2)) presents a highly distorted octahedral coordination in a Br_4O_2 chromophore. Here the Cu(2)-Br bond lengths are considerably different, of 2.492 and 2.931 Å (mean values), while the bridging phenoxo O(1) atom forms comparable bond distances with Cu (1) and Cu(2), in the range 1.970(16)-1.98(2) Å (Table 2). A similar complex using 2-naphthol instead of 5-Cl-phenol has been reported a few years ago where the Cu–Cu distance of 2.963(2) Å, is comparable to that found in **5** A and slightly shorter than values measured in **5**B and **6** (Table 2).[15]

IR and UV/Vis spectra of complexes.

The FTIR spectra of compounds **1–6** are shown in Figure S1–S6. All the complexes show bands due to C=N stretch in the region 1620–1650 cm^{-1} and skeletal vibration in the region 1445–1470 cm^{-1}. Electronic spectra of all the complexes have been studied in both MeOH and DMF medium. The complexes exhibit very comparable absorption bands in the range of 370 – 385 and 600–640 nm (Figure S7–S12). The observed lower energy weak band at around 600–640 nm may be attributed due to the d – d transition, and the corresponding strong higher energy single band (between 370 and 385 nm) is due to the LMCT. It is well known from the ORGEL diagram, that for a Cu (II) *i:e* d^9 system the electronic transition will occur from the *g.s* ^2E_g to the next *e.s* $^2T_{2g}$ and is expected to take place at around 800 nm for octahedral coordination geometry. When the J–T distortion takes place in the octahedral coordination environment the band around 800 nm undergoes a considerable blue shift corresponds to square-pyramidal and square-planar structures.[16] In the synthesized complexes (except **4**) the d – d transition positions are in a good agreement with a square-pyramidal geometry around the copper centres and in case of **4** the d-d transition further blue shifted to 600 nm, a characteristics of square planner copper(II) complex[17] as are observed in X-ray single crystal structural analyses (*vide supra*).

Solution studies: Mass spectrometry

ESI-MS spectral study has been performed to determine the composition of the multinuclear complexes (**1, 5, 6**) in MeOH (Figure S13- S18). The spectral analyses reveal that these multinuclear complexes dissociate in solution to lower nuclearity complexes. Complex **1** shows a base peak at 329. 0259 amu (calc. 329.0356 amu) which matches well with the calculated m/z value of the non brominated mono nuclear species, $[Cu(L1)]^+$. The other peak appears at 408.9359 amu may be assigned for brominated analogue of mono nuclear species, $[Cu(L1)Br]^+$ (m/z, calc. 408.9461 amu). Both the trinuclear complexes **5** and **6** dissociate similarly in solution. The complex **5** shows base peak at 328.0288 amu and another peak at 737.0067 amu where the former matches well with the mono nuclear species $[Cu(L5)]^+$ (calc. 328.0404 amu) and the latter with the dinuclear species $[Cu_2(L5)_2Br]^+$ (calc. 736.9991 amu). The peaks observed in the spectrum of **6** are at 314.0136 and 708.9736 amu which corroborate well with the mono nuclear species $[Cu(L6)]^+$ (calc. 314.0247 amu) and the dinuclear species $[Cu_2(L6)_2Br]^+$ (calc. 708.9678 amu), respectively.

EPR Study

The X-band EPR spectra of complexes **1**, **5** and **6** in solid-state, measured at 77 K, are depicted in Figure 5. The spectrum of complex **1** (Figure 5 A) shows a dissymmetric isotropic broad band having no hyperfine structure, indicating that at low temperature the copper centres in complex **1** exist in a centrosymmetric environment that leads to an isotropic limiting case. Complex **5** exhibits four hyperfine lines in its EPR spectrum, as usually observed for copper(II) complexes. From the shape of EPR signals and the calculated g values (2.44 ($g_\parallel$), 2.10 ($g_\perp$), 2.0023 (g_e)) for this complex it is clear that the unpaired electron is predominantly in the $dx^2–y^2$ orbital giving $^2B_{1g}$ as the ground state.[18] This implies that the metal–ligand bonding in complex **5** is essentially covalent. On the other hand for complex **6** (Figure 5C) the calculated g values ($g_\parallel < g_e(2.0023)$ suggests that the metal–ligand bonding has a considerable ionic character.[18]

Magnetic Study

The magnetic properties of complex **1**, in the form of $\chi_M T$ (χ_M is the susceptibility per tetrameric unit) *vs.* T plots, are shown in Figure 6 in a temperature range 2–300 K. For **1**, the $\chi_m T$ value at room temperature, 0.78emu K mol^{-1} ($\mu_{eff} = 2.50\ \mu_B$), which is close to the expected value of 0.75emu K mol^{-1} ($\mu_{eff} = 2.45\mu_B$) of four independent Copper ions ($S_{Cu(II)}$, $S_{Cu(I)}$, $S_{Cu(I)}$,$S_{Cu(II)}$) = (1/2, 0,

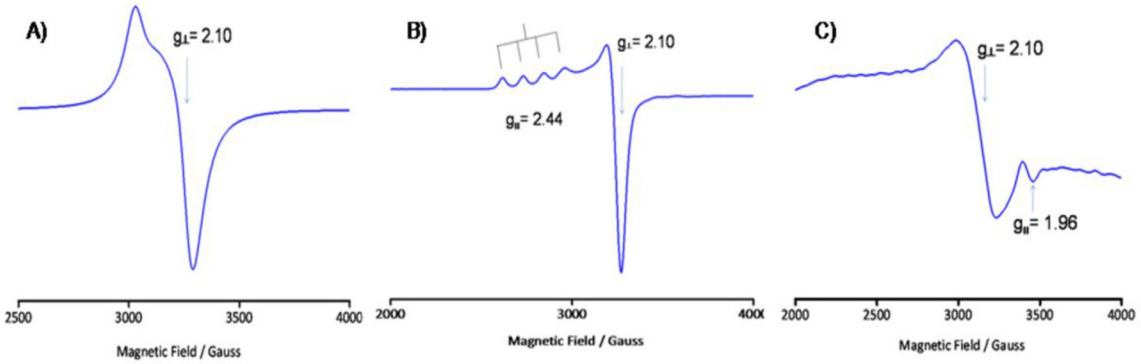

Figure 5. X-band EPR spectra of the complexes (A for complex **1**), (B for complex **5**) and (C for complex **6**) in the solid-state at 77 K.

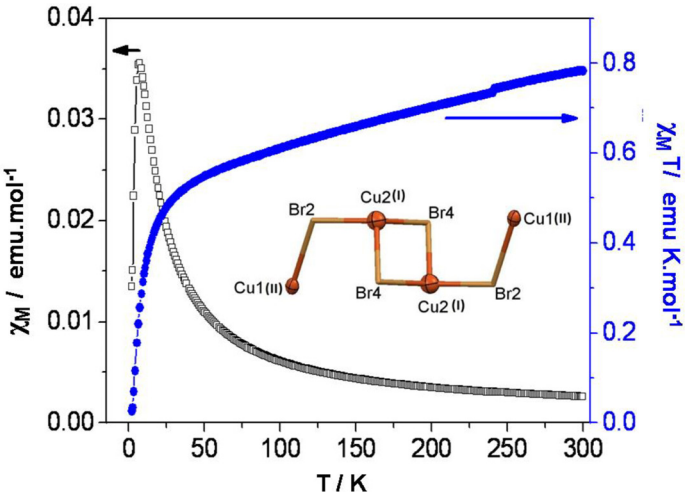

Figure 6. Temperature variation of the magnetic susceptibilities of **1** as χ_M and $\chi_M T$ versus T plots (The solid line represents the best fit of the experimental data based on the Heisenberg model).(inset-the magnetic exchange coupling pathway for complex **1.**).

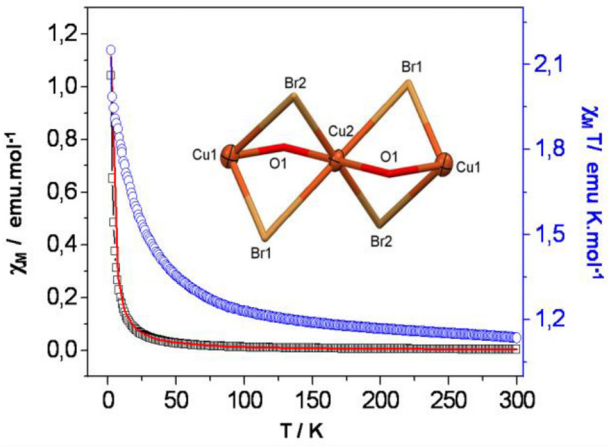

Figure 7. Temperature variation of the magnetic susceptibilities of **5** as χ_M and $\chi_M T$ versus T plots (The solid line represents the best fit of the experimental data based on the Heisenberg model).(inset-the magnetic exchange coupling pathway for complex **5.**).

0, 1/2) with g = 2.00. Upon cooling, the $\chi_m T$ value decreases continuously to a minimum of 0.02emu K mol^{-1} (μ_{eff} = 0.46μ_B) at 2 Kfor **1.** Nevertheless, from the structure of complex **1**, it should be expected the absence of any significant magnetic interaction since two Cu^{II} ions (Cu1) are connected by long –Br–Cu^{I}–Br–Cu^{I}–Br bridges (Figure 6(inset)). The presence of a weak, although noticeable antiferromagnetic interaction in complex **1** suggests that the "diamagnetic"–Br–Cu^{I}–Br–Cu^{I}–Brbridge is able to transmit such kind of magnetic interaction, as found in other long "diamagnetic"-bridges.[19-20]

The magnetic properties of complex **5** and **6** in the form of $\chi_M T$ (χ_M is the susceptibility per trimer unit) *vs.* T plots, are shown in Figure 7 and Figure 8 in a temperature range 2–300 K. For **5**, the $\chi_m T$ value at room temperature, 1.14emu K mol^{-1} (μ_{eff} = 3.02μ_B), which is close to the expected value of 1.13emu K mol^{-1} (μ_{eff} = 3μ_B) of three independent Cu(II) (S = 1/2) ions with g = 2.00. Upon cooling, the $\chi_m T$ value increases continuously to reach a value of 2.15 emu K mol^{-1} (μ_{eff} = 4.15 μ_B) at 2 K for **5**, indicating a ferromagnetic interaction between adjacent copper (II) ions. For **6**, the $\chi_m T$ value at room temper-

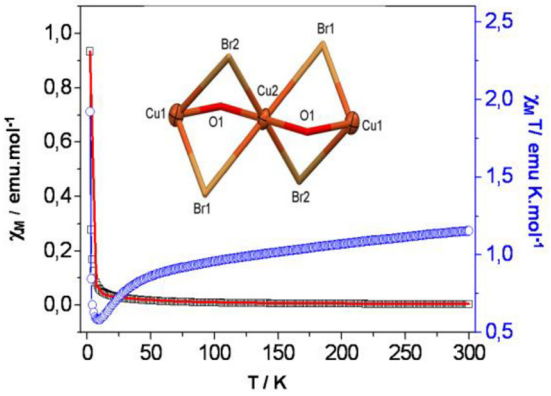

Figure 8. Temperature variation of the magnetic susceptibilities of **6** as χ_M and $\chi_M T$ versus T plots (The solid line represents the best fit of the experimental data based on the Heisenberg model). (inset-the magnetic exchange coupling pathway for complex **6**).

ature, 1.16 emu K mol^{-1} ($\mu_{eff=}$ 3.04 μ_B), which is close to the expected value of value of 1.13emu K mol^{-1} ($\mu_{eff}=3\mu_B$) of three independent Cu(II) (S = 1/2) ions with g = 2.00. Upon cooling, the $\chi_m T$ product decreases gradually to a minimum of 0.59emu K mol^{-1} (2.17 μ_B) at 10 K, then rises abruptly to a maximum of 1.92 emu K mol^{-1}(3.92 μ_B) at 2 K for **6**, indicating a dominant antiferromagnetic interaction between adjacent copper (II) ions.

The experimental magnetic susceptibility data were analysed with Eq. (1) for a symmetrical linear trinuclear copper(II) complex, assuming that the exchange constant between the neighbouring copper ions are identical ($J_{12}=J_{23}=J$) and the exchange constant between the terminal copper ions is zero. The inter-trimer exchange interaction was taken into account by using the mean field approximation Eq. (3).[21]

$$\hat{H} = -2J\,(S_1S_2 + S_2S_3) \tag{1}$$

$$\chi_t = \frac{Ng^2\mu_B^2}{4kT}\frac{1+e^{\frac{-2J}{kT}}+10e^{\frac{J}{kT}}}{1+e^{\frac{-2J}{kT}}+2e^{\frac{J}{kT}}} \tag{2}$$

$$\chi_M = \frac{\chi_t}{1-\chi_t(2zJ'/Ng^2\beta^2)} \tag{3}$$

Where χ_m denotes the magnetic susceptibility per tricopper (II), z*j* is the inter-trimer exchange parameter and the other symbols have their usual meaning. To determine the exchange parameters via the triple bridge (see Figure 7 and 8 (inset), χ_M were fitted for the range 2–300 K (solid curve in Figure 7 and Figure 8) for **5** and **6**, gives the best agreement with the experimental data for $g = 2.00$, $J = +16.64\ cm^{-1}$ and $zJ' = +0.03\ cm^{-1}$for **6** ($R^2 = 0.99651$) and g = 2.07,$J = -11.76\ cm^{-1}$, $zJ' = +0.53\ cm^{-1}$for **7** ($R^2 = 0.99879$), z the number of nearest neighbours of each trimer (z = 2, as in **5** and **6**).

There are three magnetic pathways: one phenoxo and two bromide bridges for complexes **5** and **6** (see Figure 7 and 8 (inset), Complex **5** and **6** are the first example of a linear Cu(II) trimers containing triple-mixed bromide and phenoxido bridges which have been structurally and magnetically characterized according to the CCDC database (updated Nov. 2014), and therefore, their magnetic properties cannot be compared with other similar complexes. Nevertheless, There are Cu(II) trimers and Cu(II) dimers with double-mixed chloride and phenoxo bridges which are structurally and magnetically characterized (see Table 3).

Different magnetic properties and *J* values for **5** and **6** are interesting despite the similar coordination environments and Cu–Cu distances. As can be seen in Table 3, when the Cu_2XO (X=Cl or Br) four-membered ring is close to planarity, the Cu–O–Cu and Cu–X–Cu bond angle are increase and in all cases good overlap of the Cu^{II} magnetic orbital with the orbitals of both bridging atoms gives strong antiferromagnetic interactions. Compounds **5** and **6** are folded showing small dihedral angles, Cu–O–Br–Cu [121.20°-125.41° for **5**, 122.85°-125.60° for **6** respectively. When the dihedral angle a decreases, both Cu–O–Cu and Cu–X–Cu bond angles also decrease, becoming values of around $<100°$ and $<70°$ for compounds **5** and **6.**

Table 3. Selected Structural and Magnetic Data for Compound **5**, **6** and Cu (II) Complexes with Double-mixed Chloride/Bromide and Phenoxo Bridge.

Complex	Cu–Cu (Å)	Cu-O-Cu (°)	Cu-X–Cu (°)	Cu (1)–O–X–Cu (2)	J (cm^{-1})	Ref.
5 A	2.973	98.84	67.21 68.92	121.62 122.90	+ 16.64	this work
5B	2.999	97.60	66.57 69.01	121.20 125.41		
6	2.992	98.79	67.16 69.02	122.85 125.60	–11.76	this work
$[Cu_2L(Br)]Br_2$	3.151	106.3	75.5	146.4	–34	[22]
$[Cu_3L_2(\mu\text{-}Cl)_3Cl]_3$ 0.46CH_3OH}$_n$	3.053 3.083	103.6 101.8	79.5 79.1	137.90 142.18	–44.9	[23]
$[Cu_2(mphp)Cl_3(MeOH)(H_2O)](MeOH)$	3.256	109.5	82.74	166.93	–104	[24]
$[Cu_2(py2th2\ s)Br_3]$	3.2710 3.2394	116.04 114.63	80.08 78.50	165.0	–109.5	[25]
$[Cu_2(MeO\text{-}hxtaH_2)(\mu\text{-}Cl)(CH_3OH)].3CH_3OH$	3.3071	117.3	78.06	160.28	–123	[26]
$[Cu_2(MeO\text{-}hxtaH_2)(\mu\text{-}Br)(CH_3OH)].3CH_3OH$	3.3375	118.7	75.18	160.97	–131	[26]
$[Cu_2(L\text{-}O^-)Cl]$	3.265	111.4	89.6	178.1	–167.5	[27]
$[Cu_2(L^1\text{–}O)Cl_3]$	3.293 3.270	116.23 115.18	84.81 84.84	172.0	–187	[28]

X:Cl orBr

These lower bond angles, together with the worse overlap involving the in-plane orbitals of the bridges reduce the antiferromagnetic component of the coupling, and the experimental response is becoming ferromagnetic for **5** or small antiferromagnetic for **6.**

Theoretical study

We have focused the theoretical study in three important aspects described above. First we explain the effect of the auxiliary part in bromination of the complexes as well as the regioselectivity observed in the bromination of the aromatic ring in L1 (complex **1**). Second, we have also computed the theoretical J values and spin density plots of complexes **5** and **6**, where ferro and antiferromagnetic coupling is observed respectively, despite of having very similar solid state structure. Finally, we rationalize by means of DFT calculations the auxiliary part mediated different nuclearity observed in the Cu-complexes of L1, L4, L5 and L6.

Regioselectivity of the Bromination of complex 1

Experimentally, the bromination only takes place in ligand L1 and does not occur in L2 and L3 where the C_{para} is either unsubstituted (L2) or bonded to a methyl group (L3). We have computed the atomic charges of the species (Figure 9) using L2 and L3 instead of L1 and equivalent results are obtained (see

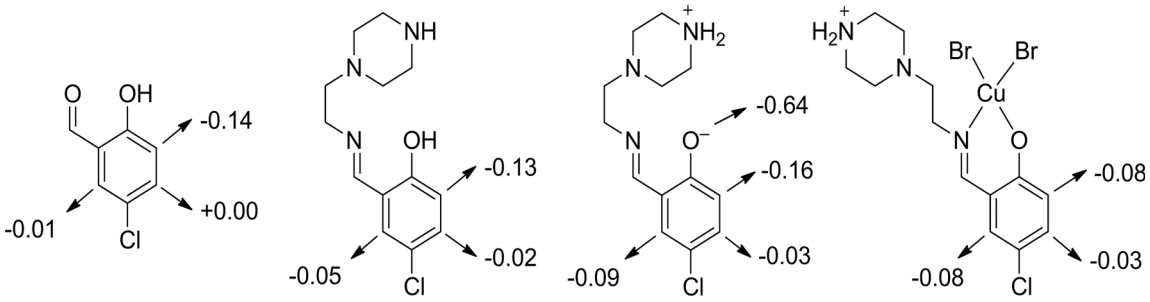

Figure 9. Merz-Kollman electron charges of several derivatives of 5-choloro salicylaldehyde.

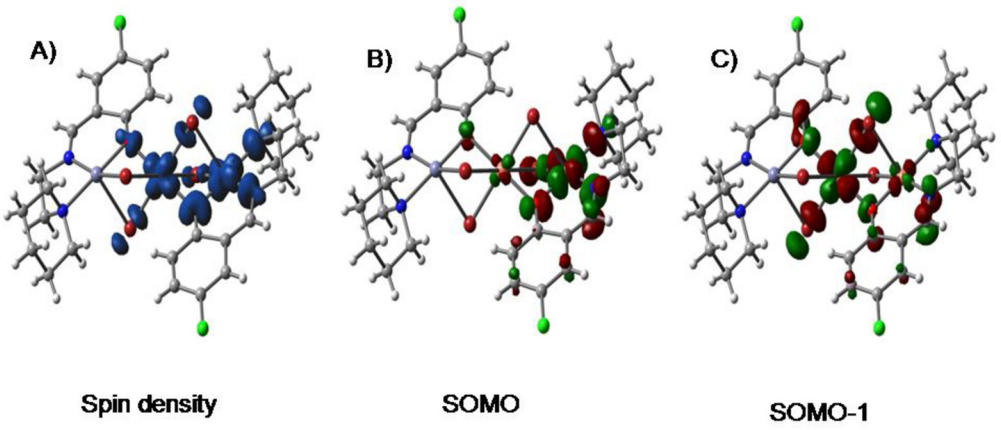

Figure 10. (A). Graphical representation of the spin density (contour 0.004 e Å^{-3}) at the ground-state (high-spin) configuration of compound **5.** (B, C) Pictorial representation of the SOMO involving the $d_{x^2-y^2}$ orbitals of Cu^{II} in compound **5.**

ESI, Figure S21). Therefore the charge distribution of the aromatic carbon atoms does not explain why the bromination is only observed in L1. However, the charge at the phenoxido O atom is slightly lesser negative in L1 (-0.64 e) mostly influenced by Cl in para position than in either L2 or L3 (-0.66 e). Consequently, a likely explanation for the bromination in L1 is that the rate of formation of the Cu complex is higher in L2 and L3 (O atom more nucleophilic) than L1 and consequently the bromination does not occur in the former ligands. Conversely, in L1 the rate of formation of the complex is slower and bromination of the ligand occurs before the metal complexation of the ligand is completed. It is known that copper (II) bromide is a simple and efficient catalyst for mono bromination of electron rich aromatic compound[29] and in general the mono-bromination takes place at the *para* position relative to the –OH, –OR or $–NR_2$ substituent and at the ortho position in case the para is blocked by an alkyl group. But in case of inorganic complexes it is very rare where organic substitution is taking place during inorganic complex synthesis. Since in L1 the *para* position is blocked by a chlorine atom and itself is an *ortho–para* directing group, we have studied the regioselectivity of the bromination. To analyse it, we have computed the ESP charges of several species that may exist in the reaction mixture upon the addition of the $CuBr_2$ reagent. They are shown in Figure 9 along with the charges at the three C atoms where the S_EAr may occur. In the three species considered where the Cu is not coordinated the activated carbon atom (more nucleophilic) is in *ortho* to the –OH group, and the other two C atoms are deactivated (negligible charge). In the specie where the metal is coordinated to the ligand, the aromatic ring is more deactivated (the charge at the C_{ortho} is reduced by half) and the bromination does not likely happen in this compound.

Magnetic study

In order to provide the magnetic coupling interactions theoretically, the spin-density distribution is analysed in compounds **5** and **6.** According to the molecular orbital theory, spin delocalization is the result of electron transfer from the magnetic centers to the ligand atoms. For compound **5**, a spin-exchange model was generated for theoretical studies using the crystal structure geometry. Calculation of the individual pair wise exchange constant has been performed by changing one Cu1 atom by a Zn atom. This procedure not only saves computational time but also was found to give accurate results (close to the experimentally fitted values) compared to the trinuclear models.[30] Spin-unrestricted DFT calculations were performed on the this model dimer [Cu2] and the theoretical *J* value is only 2.6 cm^{-1}, which confirms the ferromagnetic coupling between both metal centres. However the theoretical value underestimates the magnitude of *J* significantly, since the experimental value is 16.4 cm^{-1} (see Table 3). Mulliken spin population analysis (see Table 4) indicates that a significant spin (ca. 0.64 e) is delocalized through the ligands, and the rest (1.36 e) is carried by the Cu atoms. The spin-density plot is shown in Figure 10 A for the high-spin state of **5.** The spin-den-

Table 4. Mulliken spin densities (e) computed for the high spin configuration of the $[Cu]_2$ dimer model of compound **5.** See Figure 4 for numbering scheme

Atom label	Spin density	Atom label	Spin density
Cu1	0.67	Br2	0.10
Cu2	0.69	N1	0.09
O1	0.10	N2	0.11
Br1	0.07		

sity distribution shows a delocalization mechanism in which the Cu atoms carry 68% of the net spin and the remaining part is delocalized through coordinating atoms. The spin density is similar in the phenoxido (0.10 e) O atom and the bridging Br2 (0.10 e) atom and it is smaller in the other Br-bridged atom (Br1, 0.07 e).

In octahedral copper (II) complexes, the $d_{x^2-y^2}$ orbital contains the unpaired electron; consequently, this orbital along with the local orbitals of the bridging ligands are involved in the super-exchange pathway. This behaviour is observed in the orbital analysis of complex **5.** The SOMOs involving the $d_{x^2-y^2}$ atomic orbitals of Cu^{II} metal centers are represented in Figure 10, where the participation of the p orbitals of the O and Br atoms of phenoxide and Br bridges can also be observed. The shapes of the SOMOs and the spin density plot indicate that the bridging O atom is more effective for mediating the magnetic exchange than the Br atoms; in spite of having similar atomic spin density values (see Table 4).

Conversely to **5**, compound **6** presents antiferromagnetic exchange coupling as is more common in this type of complexes (see Table 3). The spin-exchange model was generated for the theoretical study using the crystal structure geometry. Calculation of the individual pair wise exchange constant has been performed by changing one Cu1 atom by a Zn atom. The calculated value using this procedure is $J = -16.9\ cm^{-1}$, which is in reasonable agreement with the experimental value ($-11.76\ cm^{-1}$) and confirms the antiferromagnetic coupling. In order to further examine the magnetic coupling mechanism, the spin-density distribution has been analysed. The spin density values in the broken-symmetry (LS) and high spin (HS) states are summarized in Table 5, where positive and negative

Table 5. Mulliken spin densities (e) computed for the high (HS) and low spin (LS) configurations of the $[Cu]_2$ dimer model of compound **6.** See Figure 3 for numbering scheme

Atom label	Spin density HS	Spin density LS	Atom label	Spin density HS	Spin density LS
Cu1	0.56	0.55	Br2	0.15	–0.15
Cu2	0.59	–0.58	N1	0.11	0.11
O1	0.12	0.02	N2	0.13	0.13
Br1	0.11	0.11			

signs denote α and β spin states, respectively. In Table 5 it is shown that the spin densities on the two Cu(II) ions have similar absolute values but opposite signs. The spin densities of $+0.55$ on one Cu(II) and -0.56 on the other reveals that they are indeed the magnetic centres; however, some of the spin density delocalizes onto the ligands. Moreover, the spin population analysis indicates (HS) that a significant spin (ca. 0.85 e) is delocalized through the ligands, and the rest (1.15 e) is carried by the central Cu atoms. The spin-density plot is shown in Figure 11 A for the high-spin state of **6.** The spin density (see Table 5) is slightly lower in the phenoxido (0.12 e) O atom than the Br2 (0.15 e) O atom. Interestingly, the spin carried by the phenoxido O atom is negligible in the broken-symmetry state (0.02), indicating a polarization competition between the two Cu atoms with α and β spin density, respectively.

The representation of the magnetically relevant SOMOs obtained for complex **6** are shown in Figure 11. As explained above, the $d_{x^2-y^2}$ orbital contains the unpaired electron in Cu(II) octahedral complexes; consequently, this orbital along with the local orbitals of the bridging ligands are involved in the super-exchange pathway, as confirmed in the SOMOs represented in Figure 11, where the atomic p orbitals of the bridging O and Br atoms also participate. The shapes of the SOMOs and the spin density plot indicate that the bridging O atom is more effective for mediating the magnetic exchange than the Br atoms, in

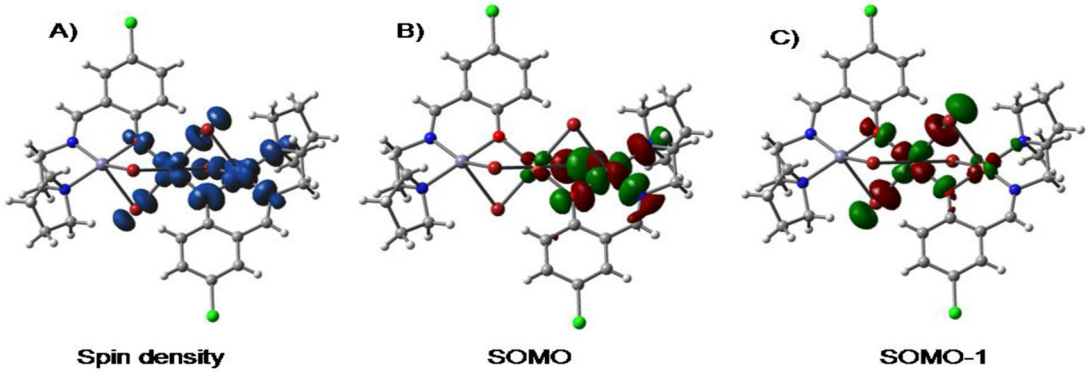

Figure 11. (A). Graphical representation of the spin density (contour 0.004 e $Å^{-3}$) at the ground-state (high-spin) configuration of compound **6.** (B,C) Pictorial representation of the SOMO involving the $d_{x^2-y^2}$ orbitals of Cu^{II} in compound **6.**

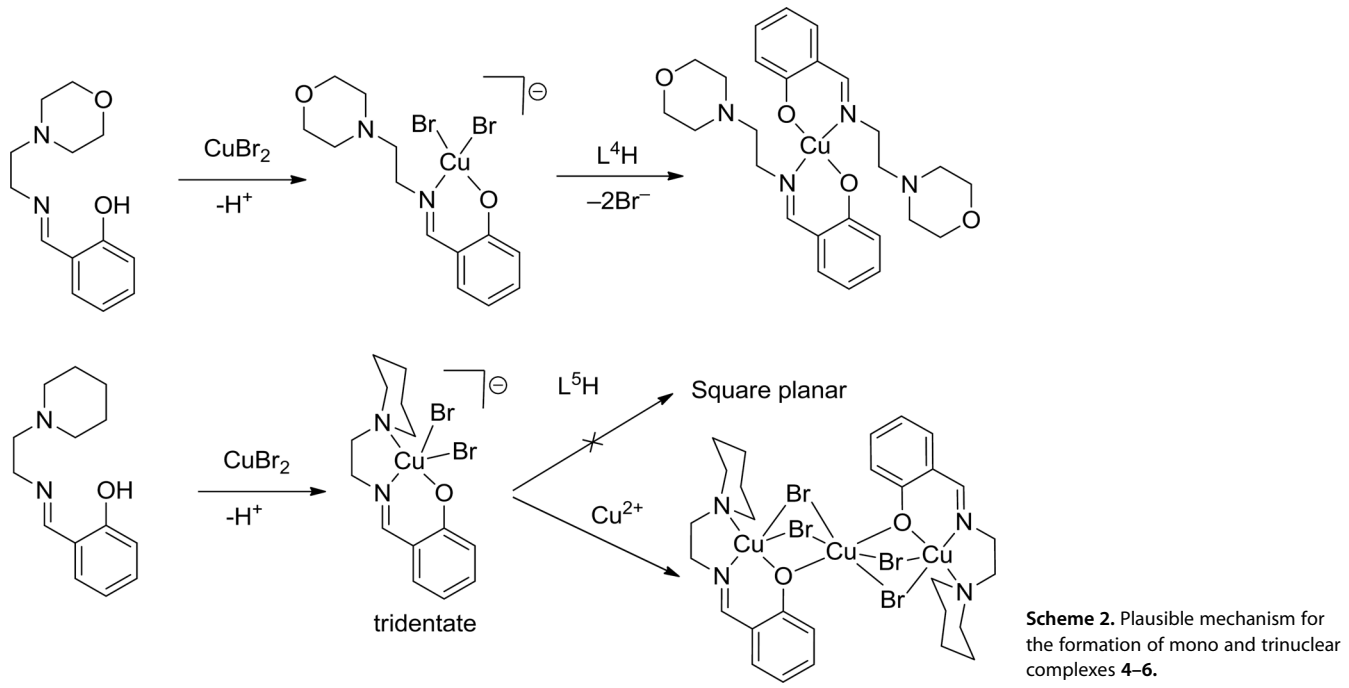

Scheme 2. Plausible mechanism for the formation of mono and trinuclear complexes **4–6.**

agreement with the low spin atomic density at the O atom in the broken-symmetry state of **6** (see Table 5)

Nuclearity study

We intend to rationalize the different nuclearity that is observed in the three Cu complexes obtained from the reaction of ligands L^4H, L^5H and L^6H (see Scheme 2) with $CuBr_2$ in MeOH. AS aforementioned, the ligands were formed in situ by reaction of 5-chloro-salicylaldehyde with the corresponding diamine and the X-ray structures of the complexes upon reaction with $CuBr_2$ are shown in Figure S20. Unexpectedly, the complex obtained using L^4H ligand is mononuclear and the other two complexes (using L^5H or L^6H) are trinuclear. Moreover, complexes **5** and **6** contain Br^- coligands in their structure.

In order to rationalize these findings we have performed DFT calculations. We have started optimizing the geometries of complexes **4–6** and, moreover, the hypothetical trinuclear complex for **4** (denoted as **4'**) and the mononuclear complexes for **5** and **6** (denoted as **5'** and **6'**). The six optimized geometries are shown in Figure. 12. The examination of the geometries shows that the formation of all complexes is possible since there is not any geometrical problem and the optimizations converge to the desired complexes. We have computed the formation energy of the trinuclear complexes **4'**, **5** and **6** from the corresponding isolated ligands, Cu^{2+} and Br^-. The relative formation energies are shown in Figure 12 (bottom). Remarkably, compounds **5** and **6** have almost identical formation energies (0.7 kcal/mol difference) and compound **4** exhibits a lesser favourable formation energy value that is $\Delta E^f_{rel} = 8.4$ kcal/mol with respect to compound **6** (the most favourable). This result strongly agrees with the experimental observation since the trinuclear complex **4'** is not formed. This difference in formation energy can be rationalized taking into consideration the N(sp^3)···Cu distance that is longer in compound **4'**, which indicates a weaker coordination bond. This also agrees with the experimental pK_a values of the piperidine (11.2), morpholine (8.3) and pyrrolidine (11.3) amines. The presence of the oxygen atom in morpholine ring reduces the pK_a in three pK_a units compared to pyrrolidine due to inductive effects. Therefore the coordination ability of the nitrogen atom of morpholine is significantly reduced compared to piperidine and pyrrolidine, thus explaining the formation of the square planar complex **4** where the morpholine ring is not involved in the Cu coordination. A plausible mechanism is proposed in Scheme 2, where in the first step the ligand acts as bidentate in **4** and as tridentate in compounds **5** and **6.** This facilitates the formation of the square planar complex in **4** but does not in **5** and **6** that crystallize as trinuclear complexes.

Conclusion

We used to overlook the impact of the atom or group of atoms, which we referred here as "auxiliary" part of a ligand on the overall coordination chemistry of a metal ion. Our present study gives us an ample opportunity to explore that untouched issue. In order to verify that impact we introduced two auxiliary parts, R and X, via our synthetic strategy to simple N,N,O-donor Schiff-bases and obtained six ligands, HL1-HL6, by combining 5-R-2-hydroxy-benzaldehyde (R = Cl/ H/ Me) and N-(2-aminoethyl)-Y (Y = piperazine/ morpholine/ piperidine/ pyrrolidine). On reaction with Cu(II)Br_2 those six ligands creates several unusual coordination chemistry. For the ligands where R is varied and X is kept fixed (HL1-HL3) the most striking observation is the bromination in aromatic ring when R=Cl. DFT calculations justify that very finding with R=Cl but not for R=H

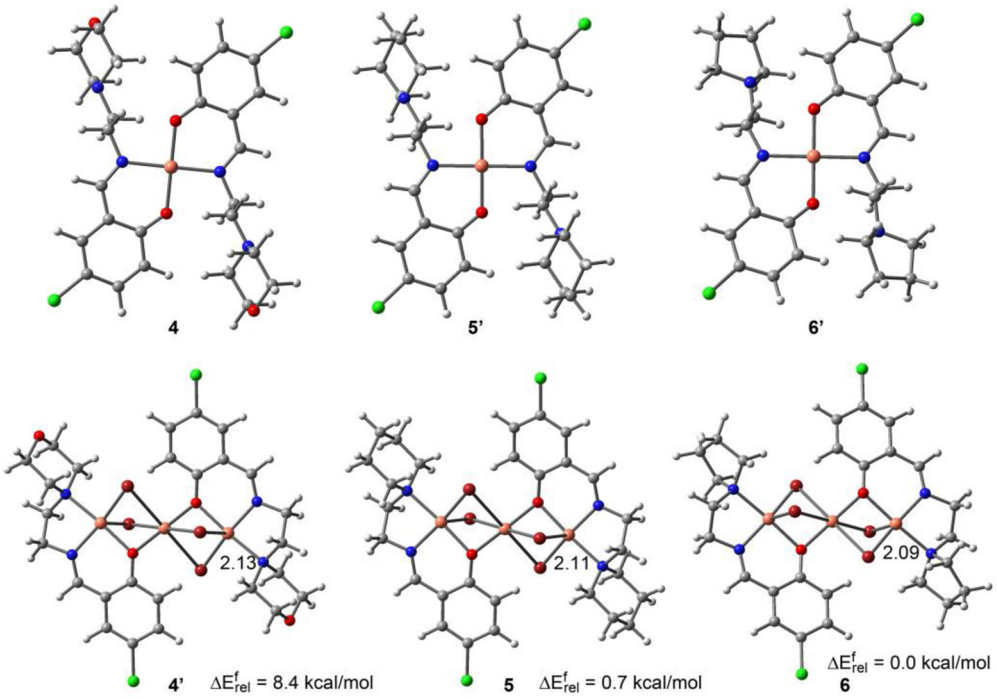

Figure 12. BP86-D3/def2-TZVP optimized complexes **4**–**6** observed experimentally and the hypothetical **4'**–**6'** complexes. Distances in Å.

or CH_3. On the other hand, when X is varied on keeping R fixed as Cl (HL1, HL4-HL6) we have encountered several unprecedented consequences like formation of varying nuclearity complexes, formation of mixed valence species and generation of ferro- and antiferromagnetic complexes. DFT calculations done on those issues corroborate well with the experimental observations. From our study it is thus verified that "auxiliary" part which according to the definition should not affect anything but visible they do.

Experimental Section

Six complexes have been prepared by adopting template synthetic technique. Typically methanolic solution of Cu(II)Br_2 is treated with the Schiff-base ligand formed in situ via condensation of 5-R-2-hydroxy-benzaldehyde (R=Cl/H/Me) and amines. Single crystals suitable for X-ray diffraction were obtained by adopting evaporation technique. These have been further detailed in the supporting information.

Acknowledgements

The authors wish to thank the University of Calcutta for providing single-crystal X-ray diffractometer, ESI-MS and SQUID-VSM facilities. AF and AB thank the MINECO of Spain for financial support (CONSOLIDER-Ingenio 2010 project CSD2010-0065, FEDER funds) and CTI (UIB) for computational facilities. IM is thankful to UGC, India [UGC/729/Jr Fellow(Sc)] for providing fellowship.

Keywords: Schiff bases · Brominated mixed valence Cu(I)-Cu(II) complex · Variable nuclearity · Magneto-structural correlation · Density functional calculations

[1] P. Braunstein, F. Naud, *Angew. Chem. Int. Ed.* **2001**, *40*, 680.
[2] R. Mukherjee, *Coord. Chem. Rev.* **2000**, *203*, 151.
[3] R. Dorta, E. D. Stevens, N. M. Scott, C. Costabile, L. Cavallo, Carl D. Hoff, S. P. Nolan, *J. Am. Chem. Soc.* **2005**, *127*, 2485.
[4] K. D. Benkstein, J. T. Hupp, C. L. Stern, *J. Am. Chem. Soc.* **1998**, *120*, 12982.
[5] P. Chakraborty, J. Adhikary, S. Samanta, D. Escudero, A. C. Castro, M. Swart, S. Ghosh, A. Bauzá, A. Frontera, E. Zangrando, D. Das, *Cryst.-Growth Des.* **2014**, *14*, 4111.
[6] P. Chakraborty, J. Adhikary, R. Sanyal, A. Khan, K. Manna, S. Dey, E. Zangrando, A. Bauzá, A. Frontera, D. Das, *Inorg. Chim. Acta.* **2014**, *421*, 364.
[7] X.-M. Zhang, M.-L. Tong, X.-M. Chen, *Angew. Chem. Int. Ed.* **2002**, *41*, 1029.
[8] L. C. King, G. K. Ostrum, *J. Org. Chem.* **1964**, *19*, 3459.
[9] P. Kovacic, K. E . Davis, *J. Org. Chem.* **1964**, *86*, 427.
[10] R. Rodebaugh, J. S. Debenham, B. F. Reid, J. P. Snyder, *J. Org. Chem.* **1999**, *64*, 1758.
[11] R. W. Evans, J. R. Zbieg, S. Zhu, W. Li, D. W. C. MacMillan, *J. Am. Chem. Soc.* **2013**, *135*, 16074.
[12] A. W. Addison, T. N. Rao, J. Reedijk, J. V. Rijn, G. C. Verschoor, *J. Chem. Soc. Dalton Trans.* **1984**, 1349.
[13] Y. L. Sang, X. S. Lin. , *Russ. J. Coord. Chem.* **2010**, *36*, 472.
[14] a) S.-P. Xu, L. Shi, P.-C. Lv, R.-Q. Fang, H.-L. Zhu, *J. Coord. Chem.* **2009**, *62*, 2048; b) Z.-Lu. You, P. Hou, C. Wang, *J. Coord. Chem.* **2009**, *62*, 593; c) S.-S. Qian, D.-M. Xian, Z.-L. You, H.-L. Zhu, *Synth. React. Inorg., Met.-Org., Nano-Met. Chem.* **2013**, *43*, 972.
[15] Y.-L. Sang, X.-S. Lin , *Transition Met. Chem.* **2009**, ***34***, 931.
[16] A. B. P. Lever, Inorganic Electronic Spectroscopy; Elsevier: Amsterdam, The Netherlands, **1984**, pp 553.
[17] A. B. P. Lever, Inorganic Electronic Spectroscopy; Elsevier: Amsterdam, The Netherlands, **1984**, pp 570.
[18] T. M.A. Ismail, A. A. Saleh, M. A. Ghamry, *Spectrochimica Acta Part A.* **2012**, *86*, 276.

[19] E. Colacio, R. Kiveka, F. Lloret, M. Sunberg, J.' Suarez-Varela, M. Bardaji', A. Laguna, *Inorg. Chem.* **2002**, *41*, 5141.
[20] F. Thetiot, S. Triki, J. Sala-Pala, *New J. Chem.* **2002**, *26*, 196.
[21] O. Kahn, Molecular Magnetism, VCH Publishers, **1993.**
[22] C. J. O'Connor, D. Firmin, A. K. Pant, B. Ram Babu, E. D. Stevensla, *Inorg. Chem.* **1986**, *25*, 2300.
[23] A. Biswas, M. G. B. Drew, C. J. Gomez-Garcıa, A. Ghosh, *Inorg. Chem*. **2010**, *49*, 8155.
[24] J. Tang, J. S. Costa, A. Pevec, B. Kozlevcar, C. Massera, O. Roubeau, I. Mutikainen, U. Turpeinen, P. Gamez, J. Reedijk, *Crystal Growth & Design*, **2008**, *8*, 1005.
[25] I. A. Koval, M. Huisman, A. F. Stassen, P. Gamez, O. Roubeau, C. Belle, J. L. Pierre, E.
Saint-Aman, M. Luken, B. Krebs, M. Lutz, A. L. Spek, J. Reedijk, *Eur. J. Inorg.Chem.* **2004**, 4036.
[26] S. Laborda, R. Clerac, C. E. Anson, A. K. Powell, *Inorg. Chem*. **2004**, *43*, 5931.
[27] K. D. Karlin, A. Farooq, J. C. Hayes, B. I. Cohen, T. M. Rowe, , E. Sinn, J. Zubieta, *Inorg. Chem.* **1987**, *26*, 1271.
[28] S. P. Foxon, D. Utz, J. Astner, S. Schindler, F. Thaler, F. W. Heinemann, G. Liehr, J. Mukherjee, V. Balamurugan, D. Ghosh, R. Mukherjee, *Dalton Trans.* **2004**, 2321.
[29] S. Bhatt, S. K. Nayak, *Synth. Commun.* **2007**, *37*, 1381.
[30] a) E. Ruiz, A. Rodríguez-Fortea, J. Cano, S. Alvarez, P. J. Alemany, *Comput. Chem.* **2003**, *24*, 982; b) E. Ruiz, S. Alvarez, J. Cano V. J. Polo, *Chem. Phys.* **2005**, *123*, 164110.

Submitted: December 16, 2015
Accepted: March 10, 2016